IOP Publishing Journal of Optics

J. Opt. **13** (2011) 115701 (15pp) doi:10.1088/2040-8978/13/11/115701

Optical polarization evolution near a non-Hermitian degeneracy

M V Berry

H H Wills Physics Laboratory, Tyndall Avenue, Bristol BS8 1TL, UK

E-mail: asymptotico@physics.bristol.ac.uk

Received 15 August 2011, accepted for publication 8 September 2011
Published 13 October 2011
Online at stacks.iop.org/JOpt/13/115701

Abstract
Recent insights into the time development of quantum states driven by non-Hermitian matrices, and an exactly solvable model, can be applied to the evolution of optical polarization in a stratified nontransparent dielectric medium twisted cyclically along the propagation direction. The twist is chosen to encircle a degeneracy (branch-point) in the plane of parameters describing the medium. Polarization evolutions are determined analytically and illustrated as tracks on the Poincaré sphere and the stereographic plane. Even when the twist is slow, the exact evolutions differ sharply from those of the local eigenpolarizations and can display extreme sensitivity to initial conditions. Underlying these dramatic violations of adiabatic intuition are the disparity of exponentials and the Stokes phenomenon of asymptotics.

Keywords: propagation, two-state, adiabatic, exceptional point, crystal optics, asymptotics, Stokes phenomenon

1. Introduction

It is now widely recognized that the mathematical differences between Hermitian and non-Hermitian operators, especially near degeneracies, have implications in several areas of physics [1, 2]. My purpose here is to show how the recently discovered dramatic violation of adiabatic intuition in quantum states driven by a changing non-Hermitian operator [3] has equally striking consequences for the propagation of the polarization state of light.

We envisage polarized light in a stratified nontransparent biaxially anisotropic dielectric medium ('crystal') whose properties vary cyclically along the beam path. The cyclic variation constitutes a loop, in the space of crystal parameters, that encloses a degeneracy where the two local polarization states (eigenvectors of the dielectric matrix: the eigenpolarizations) coincide. Because the medium is not transparent, the dielectric matrix is non-Hermitian, and the degeneracy is a branch-point, often called an 'exceptional point' [4], or, in crystal optics, a 'singular axis' [5, 6]. By analogy with the adiabatic theorem for Hermitian evolution [7, 8], it might be thought that when the medium's variation is slow the polarization of the light should follow the eigenpolarizations of the medium. In particular, at the end of the cycle the original polarization of each of the two states should return to that of the other (adiabatic'flip' [3]), reflecting the branch-point nature of the degeneracy.

Although one of the states does flip in this way, its evolution during the cycle departs wildly from the naively expected adiabatic clinging, and the other state does not flip at all. Recent progress [3] in understanding of analogous quantum problems implies that the polarization evolution is strongly dependent on the geometry (e.g. the radius) of the loop, even for very slow variations. This paper explores these variations.

Section 2 sets up the optical formalism. A major simplification is to study the evolving polarization state alone, ignoring the changes in the intensity of the light. This means that instead of solving the linear equation for the two transverse electric field components (analogous to the Schrödinger equation for a two-state quantum system), we study the nonlinear equation governing the ratio of the two components. This complex number w has a simple interpretation: w is the stereographic projection of the unit Stokes 3-vector $\boldsymbol{r}$ representing polarization on the Poincaré sphere [9, 10]. Throughout this paper we make extensive use of both the w plane and the $\boldsymbol{r}$ sphere to display the polarization evolutions. It is interesting to note that Poincaré employed w in most of his studies of polarization optics, and only discovered his now-familiar sphere much later (see [11], especially p277ff).

Section 3 introduces a local model for crystal optics near an isolated non-Hermitian degeneracy (for background,

see [6]), and a family of loops for which the evolution can be solved exactly. This is a special case of recently discovered solutions [12] for the evolving two-component vector, here adapted to give an exact explicit formula for the evolution of the polarization for arbitrary initial state. There is a special periodic solution for which the final and initial polarizations are related by a Möbius transformation. Appendix A shows how the model can be interpreted as a nontransparent perturbation of a Hermitian operator describing a transparent anisotropic crystal that is twisted along the propagation direction. The known exact solution for evolution in this Hermitian model is briefly recapitulated in appendix B; it is the same as the Rabi solution for a cycled spin [13] and resembles the precession and nutation of a heavy symmetrical top [14–16].

In section 4 the case of slow evolution is examined, by studying the exact evolution of the polarizations that start in each of the two eigenpolarizations along the propagation direction. The wild fluctuations in the final polarization of one of these states, persisting into the adiabatic limit, are described, and the dramatic discrepancies during the evolution of the other are illustrated by tracks in the stereographic plane and on the Poincaré sphere. These departures from adiabatic intuition are consequences of the Stokes phenomenon of asymptotics [17, 18]—an unanticipated connection between two areas in which Stokes made seminal contributions.

Section 5 compares the exact evolution with successively higher 'superadiabatic' [19, 20] approximations. For sufficiently high orders, the exact evolving polarizations do, as expected, cling closer to the higher approximations for most of the cycle. But they do not eliminate the final-state fluctuations in one of the polarizations. And in the other they leave oscillations near the middle of the cycle, with the polarization coiling and looping in a way that can be described precisely as discussed in appendix C; the coils persist far into the adiabatic regime. The exact evolutions starting in successive superadiabatic orders close to one of the two eigenpolarizations are very different, showing that the polarization evolutions near a non-Hermitian degeneracy can be astonishingly sensitive to initial conditions.

The concluding section 6 includes an assessment of the possibilities for observing these and related recently predicted polarization phenomena associated with non-Hermitian degeneracies.

2. Optical formalism

For a dielectric medium varying only along the propagation direction z, the electric $\boldsymbol{D}$ vector is transverse, that is

$$\boldsymbol{D}(z) = \begin{pmatrix} D_x(z) \\ D_y(z) \end{pmatrix}, \tag{2.1}$$

and for free-space wavenumber k Maxwell's equations reduce exactly to

$$\partial_z^2(\boldsymbol{\eta}(z)\cdot\boldsymbol{D}(z)) + k^2\boldsymbol{D}(z) = 0. \tag{2.2}$$

Here $\boldsymbol{\eta}$ is the transverse part of the reciprocal dielectric tensor $\boldsymbol{\varepsilon}$, that is

$$\boldsymbol{\eta}(z) = \begin{pmatrix} \eta_{xx}(z) & \eta_{xy}(z) \\ \eta_{yx}(z) & \eta_{yy}(z) \end{pmatrix} = \left(\varepsilon_0\boldsymbol{\varepsilon}(z)^{-1}\right)_\perp . \tag{2.3}$$

It will suffice to consider weak and gentle anisotropy, so we write

$$\begin{gathered} \boldsymbol{D}(z) = \exp(\mathrm{i}kz)\boldsymbol{d}(z), \qquad \boldsymbol{\eta}(z) = (\boldsymbol{I} + \delta\boldsymbol{\eta}(z)), \\ \operatorname{Tr}\delta\boldsymbol{\eta}(z) = 0, \qquad \frac{1}{k}\partial_z||\delta\boldsymbol{\eta}(z)|| \ll ||\delta\boldsymbol{\eta}(z)|| \ll 1. \end{gathered} \tag{2.4}$$

Then propagation is paraxial (back reflections are negligible), and (2.2) can be approximated by

$$\frac{2\mathrm{i}}{k}\partial_z\boldsymbol{d}(z) = \delta\boldsymbol{\eta}(z)\boldsymbol{d}(z). \tag{2.5}$$

Paraxiality is more subtle than this brief and customary argument suggests. The neglect of reflections requires that the effect of a term $\partial_{zz}\boldsymbol{d}/k^2$ be negligible. This is only true for solutions of (2.2) with initial conditions corresponding to waves travelling forwards—i.e. not a superposition of forward and backward waves. I have confirmed by numerical computation that all the solutions of (2.5) studied in the rest of this paper are close to the corresponding solutions of (2.2); the deviations take the form of weak fast oscillations that get smaller as k (suitably scaled with z to leave (2.5) invariant) increases.

The stipulation in (2.4) that the dielectric variations are traceless is made only to simplify later formulae; any non-zero trace, even if it is z dependent, simply contributes an overall scalar factor to $\boldsymbol{d}(z)$ and affects the evolution of intensity but not the polarization.

Let L be the cycle length (pitch) of the medium variation. Then it is convenient to change the evolution variable from z to an angle θ. Also, to conform to common optics convention, it is convenient to transform from the Cartesian basis $\boldsymbol{d}$ to a basis $|\psi\rangle$ of circular polarizations. Thus we define

$$\begin{gathered} z = \frac{L\theta}{2\pi}, \qquad K = \frac{kL}{2\pi}, \\ \boldsymbol{d}(z) = \boldsymbol{U}|\psi(\theta)\rangle, \qquad |\psi(\theta)\rangle = \begin{pmatrix} \psi_1(\theta) \\ \psi_2(\theta) \end{pmatrix}, \\ \delta\boldsymbol{\eta}(z) = \boldsymbol{U}\boldsymbol{\Omega}(\theta)\cdot\boldsymbol{\sigma}\boldsymbol{U}^{-1}, \qquad \boldsymbol{U} = \frac{1}{\sqrt{2}}\begin{pmatrix} 1 & 1 \\ \mathrm{i} & -\mathrm{i} \end{pmatrix}, \end{gathered} \tag{2.6}$$

in which $\boldsymbol{\sigma}$ is the vector operator whose components are the three Pauli matrices, and the stratified medium is represented by the vector $\boldsymbol{\Omega}(\boldsymbol{\theta})$. In the adiabatic regime $kL \gg 1$ that we will be interested in, the new parameter K is large. With all these transformations, (2.4) becomes

$$\frac{2\mathrm{i}}{K}\partial_\theta|\psi(\theta)\rangle = \boldsymbol{\Omega}(\theta)\cdot\boldsymbol{\sigma}|\psi(\theta)\rangle. \tag{2.7}$$

This form of writing deliberately evokes the formal equivalence with two-state quantum physics, in which the θ dependent vector

$$\boldsymbol{\Omega}(\theta) = (\Omega_1(\theta), \Omega_2(\theta), \Omega_3(\theta)) \tag{2.8}$$

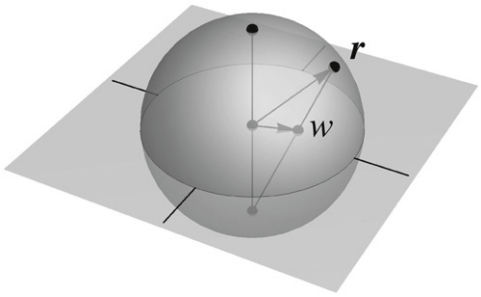

Figure 1. Stereographic projection from the unit Stokes vector $\boldsymbol{r}$ on the Poincaré sphere to the complex w plane.

represents the driving Hamiltonian: for an evolving spin in NMR, $\boldsymbol{\Omega}$ is the time-dependent magnetic driving field. For a transparent medium, the components of $\boldsymbol{\Omega}$ are real, reflecting the hermiticity of the Hamiltonian; but our emphasis will be on the non-Hermitian situation, in which $\boldsymbol{\Omega}$ is a complex vector.

The final transformation is to eliminate any scalar multipliers in the state, by defining the complex quantity

$$w(\theta) = \frac{\psi_2(\theta)}{\psi_1(\theta)}, \tag{2.9}$$

representing the polarization. Thus, the two orthogonal circular polarizations $|\psi\rangle = \mathrm{col}(1,0)$ and $|\psi\rangle = \mathrm{col}(0,1)$ correspond to $w = 0$ and $w = \infty$ respectively, and linear polarizations correspond to the unit circle $|w| = 1$. The more familiar representation of polarization as a unit Stokes vector on the Poincaré sphere, whose north and south poles correspond to the circular polarizations and whose equator represents linear polarizations, can be expressed in terms of w by

$$\begin{aligned}\boldsymbol{r}(\theta) &= \frac{1}{1+|w(\theta)|^2}(2\,\mathrm{Re}\,w(\theta), 2\,\mathrm{Im}\,w(\theta), 1-|w(\theta)|^2)\\ &= (r_1, r_2, r_3).\end{aligned} \tag{2.10}$$

(In quantum physics, $\boldsymbol{r}$ represents the state on the Bloch sphere; mathematically, it is called the Riemann sphere.) As figure 1 illustrates, w is the south-pole stereographic projection of $\boldsymbol{r}$. The evolution of states of polarization can thus be represented as tracks on the w plane or on the $\boldsymbol{r}$ sphere. Although, as we will see, some care must be taken when interpreting pictures of $w(\theta)$, this representation is very convenient for calculation, and has proved useful not only in crystal optics [6, 21] but also the polarization of daylight in the sky [22].

In terms of w, the vector evolution equation (2.7), for the two complex components of $|\psi\rangle$, becomes the following significantly simpler (albeit nonlinear) equation (of Riccati type) for the single complex polarization scalar w:

$$\partial_\theta w = \tfrac{1}{2}\mathrm{i}K((\Omega_1 - \mathrm{i}\Omega_2)w^2 + 2\Omega_3 w - (\Omega_1 + \mathrm{i}\Omega_2)). \tag{2.11}$$

In what follows, the components of $\boldsymbol{\Omega}$ will be θ-dependent (as well as complex). If they are not θ-dependent—that is, if the medium is uniform—the polarizations that propagate unchanged correspond to zeros of the right-hand side of (2.11). These are the eigenpolarizations of the operator $\boldsymbol{\Omega}\cdot\boldsymbol{\sigma}$ in the Schrödinger representation (2.7), namely

$$\begin{aligned}w_\pm &= \frac{-\Omega_3 \pm \sqrt{\Omega_1^2+\Omega_2^2+\Omega_3^2}}{\Omega_1 - \mathrm{i}\Omega_2}\\ &= \exp\left(\frac{1}{2}\mathrm{i}\beta\right)[\tan\alpha, -\cot\alpha],\end{aligned} \tag{2.12}$$

where α and β are the polar angles of $\boldsymbol{\Omega}$ (complex in the non-Hermitian cases we are interested in here.)

In this paper our interest will focus on the polarization state of the light, rather than its intensity

$$I(\theta) = \langle\psi(\theta)|\psi(\theta)\rangle = |\psi_1(\theta)|^2 + |\psi_2(\theta)|^2. \tag{2.13}$$

Nevertheless, it is worth noting how the evolution of the intensity depends on that of the polarization. The intensity also depends on the imaginary part $T(\theta) = \mathrm{Im\,Tr}\,\delta\boldsymbol{\eta}(\theta)$ of the trace of the dielectric tensor; for a lossy material, $T < 0$, and for gain $T > 0$. Including $T(\theta)$, the intensity is given by

$$\begin{aligned}I(\theta) &= I(0)\exp\left(K\int_0^\theta \mathrm{d}\theta'(\tfrac{1}{2}T(\theta') + \boldsymbol{r}(\theta')\cdot\mathrm{Im}\,\boldsymbol{\Omega}(\theta'))\right)\\ &= I(0)\exp\left\{K\int_0^\theta \mathrm{d}\theta'\left(\frac{1}{2}T(\theta') + \frac{1}{1+|w(\theta')|^2}\right.\right.\\ &\quad\times[(1+|w(\theta')|^2)\,\mathrm{Im}\,\Omega_3(\theta') + 2(\mathrm{Re}\,w(\theta')\,\mathrm{Im}\,\Omega_1(\theta')\\ &\quad\left.\left.+\,\mathrm{Im}\,w(\theta')\,\mathrm{Im}\,\Omega_2(\theta'))]\right)\right\}.\end{aligned} \tag{2.14}$$

For completeness, here is the evolution equation for the Poincaré sphere polarization vector $\boldsymbol{r}$:

$$\partial_\theta \boldsymbol{r} = K(\mathrm{Re}\,\Omega\times\boldsymbol{r} + \boldsymbol{r}\times\mathrm{Im}\,\Omega\times\boldsymbol{r}). \tag{2.15}$$

3. Model and exact solution

For the matrix representing the varying medium, we choose

$$\boldsymbol{\Omega}(\theta)\cdot\boldsymbol{\sigma} = \mathrm{i}\mu\begin{pmatrix}0 & 1\\ \rho\exp(\mathrm{i}\theta) & 0\end{pmatrix}, \tag{3.1}$$

with $\mu \ll 1$ to ensure the dielectric variations are weak. This is obviously non-Hermitian and, regarded as a family of matrices in the plane

$$z = \rho\exp(\mathrm{i}\theta) = \xi + \mathrm{i}\eta, \tag{3.2}$$

possesses a degeneracy at the origin $\rho = 0$, whose influence on the evolution is the focus of our interest. The variation of the medium along the propagation direction corresponds to a loop of radius ρ, centred on the degeneracy. In appendix A it is shown how (3.1) can be embedded in a wider family of dielectric matrices, representing initially transparent materials that are nontransparently perturbed (see [6] for more background on the relevant crystal optics). Polarization evolution for the more familiar transparent (Hermitian) case is summarized in appendix B.

The evolution generated by (3.1) has been extensively studied recently [12], using a slightly more general model in which the degeneracy need not lie at the centre of the loop and can even be outside it. But (3.1) will suffice for our purpose

here, of illustrating the sensitivity and non-adiabaticity of the evolution of the polarization. To get the simplest form of the evolution equation (2.11), we use the scaling

$$w \to \frac{2}{K\mu} w, \qquad \rho \to \frac{4}{K^2\mu^2}\rho. \tag{3.3}$$

Thus (2.11) becomes

$$\partial_\theta w = \rho \exp(\mathrm{i}\theta) - w^2. \tag{3.4}$$

With the scaling (3.3), the adiabatic regime $K \gg 1$ corresponds to loops with $\rho \gg 1$.

As can be confirmed by direct substitution using standard formulae [23], or from the solution in [12], this can be solved exactly in terms of Bessel functions J and Y. With initial condition $w_0 = w(0)$, the solution is

$$\begin{aligned} w(\theta) &= \partial_\theta \log A(\theta) \\ &= -\mathrm{i}\sqrt{\rho}\exp\left(\frac{1}{2}\mathrm{i}\theta\right)\frac{B(\theta)}{A(\theta)}, \end{aligned} \tag{3.5}$$

in which, with the definitions

$$\zeta_0 = 2\sqrt{\rho}, \qquad \zeta(\theta) = 2\sqrt{\rho}\exp(\tfrac{1}{2}\mathrm{i}\theta), \tag{3.6}$$

$A(\theta)$ and $B(\theta)$ are given by

$$\begin{aligned} A(\theta) &= (\mathrm{i}w_0 Y_0(\zeta_0) - \sqrt{\rho}Y_1(\zeta_0))J_0(\zeta(\theta)) \\ &\quad - (\mathrm{i}w_0 J_0(\zeta_0) - \sqrt{\rho}J_1(\zeta_0))Y_0(\zeta(\theta)) \\ B(\theta) &= (\mathrm{i}w_0 Y_0(\zeta_0) - \sqrt{\rho}Y_1(\zeta_0))J_1(\zeta(\theta)) \\ &\quad - (\mathrm{i}w_0 J_0(\zeta_0) - \sqrt{\rho}J_1(\zeta_0))Y_1(\zeta(\theta)). \end{aligned} \tag{3.7}$$

To get a compact representation for the final polarization state, we use the continuation formulae (section 10.11 of [23])

$$\begin{aligned} J_0(u\exp(\mathrm{i}\pi)) = J_0(u), \qquad J_1(u\exp(\mathrm{i}\pi)) = -J_1(u) \\ Y_0(u\exp(\mathrm{i}\pi)) = Y_0(u) + 2\mathrm{i}J_0(u), \\ Y_1(u\exp(\mathrm{i}\pi)) = -Y_1(u) - 2\mathrm{i}J_1(u), \end{aligned} \tag{3.8}$$

in which the second terms in the third and fourth formulae will play a significant role later. With use of the Wronskian relation (10.5.2 of [23]) between the Bessel functions, we obtain

$$\begin{aligned} w_f = w(2\pi) &= w_0 \\ &\times \frac{(1 - 2\pi\mathrm{i}\sqrt{\rho}J_1(\zeta_0)(J_0(\zeta_0) + \mathrm{i}\frac{\sqrt{\rho}}{w_0}J_1(\zeta_0)))}{(1 + 2\pi w_0 J_0(\zeta_0)(J_0(\zeta_0) + \mathrm{i}\frac{\sqrt{\rho}}{w_0}J_1(\zeta_0)))}. \end{aligned} \tag{3.9}$$

The formulae (3.5)–(3.9) enable easy evaluation of the polarization evolution and final state corresponding to any initial condition w_0. As we will see, the evolutions depend interestingly and sometimes very sensitively on the loop radius ρ.

For each loop, there is one important special solution, in which the polarization returns exactly, that is $w_f = w_0$. It corresponds to the known (and in this model degenerate) Floquet solution [12], with initial condition and evolution

$$\begin{aligned} w_0 = w_f &= -\mathrm{i}\sqrt{\rho}\frac{J_1(\zeta_0)}{J_0(\zeta_0)}, \\ w(\theta) &= -\mathrm{i}\sqrt{\rho}\exp\left(\frac{1}{2}\mathrm{i}\theta\right)\frac{J_1(\zeta(\theta))}{J_0(\zeta(\theta))}. \end{aligned} \tag{3.10}$$

From this it is clear that whenever ζ_0 corresponds to a zero of J_0 or J_1 the corresponding initial polarization is purely circular, and these situations alternate as ρ increases.

Figure 2(a) shows this periodic evolution on the Poincaré sphere, for the sample value $\rho = 12$. The two rapid changes of direction in the southern hemisphere indicate a nearby value of ρ (close to 10.2 in this case) at which the polarization track acquires self-intersections. These turns are not immediately evident in the stereographic plot of figure 2(b), and it is also difficult to discern them in the graphs of $\Re w$ and $\Im w$ of figure 2(c). But in the antipodal stereographic plot, of $-1/w^*(\theta)$ rather than $w(\theta)$, corresponding to $-\boldsymbol{r}(\theta)$ rather than $\boldsymbol{r}(\theta)$, the turns are obvious. This indicates that care must be taken when interpreting the stereographic plots to follow, especially near the south pole $|w| \gg 1$.

Regarded as a map from w_0 to $w(\theta)$, the solution (3.5)–(3.7) can be interpreted as an evolving Möbius transformation [24]. The solution (3.9), from w_0 to w_f is a parabolic Möbius transformation, with the special property that it has a single fixed point; for more general cycles, such as the excentric loops considered in [12], the corresponding Möbius transformation has a pair of fixed points. The known structure of such maps under iteration [24] therefore has a physical interpretation: it describes the changes in polarization during propagation through many repetitions of the medium (3.1).

4. Slowly changing medium

The local eigenpolarizations of our model (3.1) (special cases of 2.12) are the zeros of the right-hand side of (3.4), that is

$$w_{\mathrm{ad}\pm}(\theta) = \pm\sqrt{\rho}\exp(\tfrac{1}{2}\mathrm{i}\theta). \tag{4.1}$$

As θ increases from 0 to 2π, these trace out complementary semicircles, corresponding to half parallels of latitude on the Poincaré sphere, with each ending where the other begins; this is the 'flip' reflecting the branch-point at the degeneracy [1, 3]. As the loop radius ρ increases from zero to infinity, the semicircles migrate from the north pole to the south pole on the Poincaré sphere. The angle on the Poincaré sphere between the two eigenpolarizations is $4\arctan(\sqrt{\rho})$ for $\rho \leqslant 1$ and $4\arctan(1/\sqrt{\rho})$ for $\rho > 1$. Only for $\rho = 1$ are the states orthogonal. For all other values, the states are nonorthogonal, reflecting the non-Hermiticity of (3.1); and at the degeneracies, that is $\rho = 0$ or ∞, the states coincide, both being circularly polarized.

In this section we will study the exact evolutions $w_\pm(\theta)$ (solutions of (3.4)) that start in these eigenpolarizations, that is, the evolutions (3.5)–(3.7) with initial conditions

$$w_\pm(0) = w_{0\mathrm{ad}\pm} = w_{\mathrm{ad}\pm}(0) = \pm\sqrt{\boldsymbol{\rho}}. \tag{4.2}$$

In the adiabatic regime $\rho \gg 0$, it might be expected that the tracks of these exact evolutions will closely approximate the semicircles represented by (4.1).

However, as figure 3 illustrates, the exact and adiabatic polarization tracks are wildly discordant, and in different ways for the evolutions $w_+(\theta)$ and $w_-(\theta)$. For $w_+(\theta)$, the exact and adiabatic tracks are similar for most of the cycle but diverge

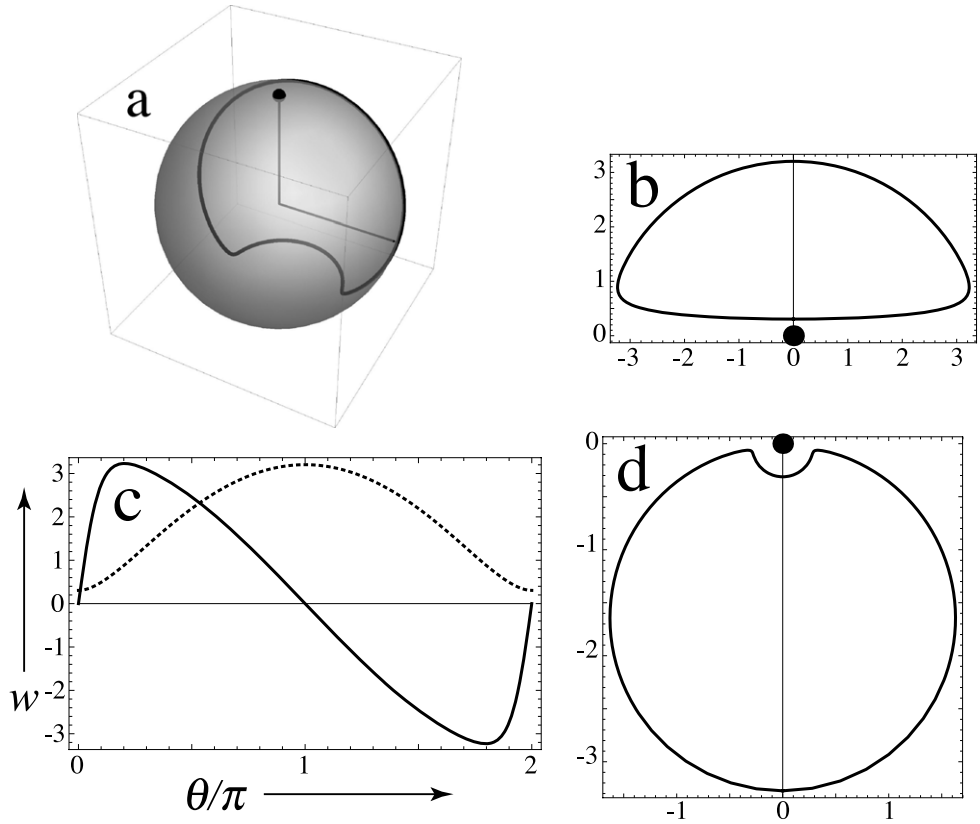

Figure 2. Representations of periodic polarization evolution $w(\theta)$ (equation (3.10)) for $\rho = 12$. (a) Track on Poincaré sphere, with filled circle indicating the north pole and lines indicating the positive r_1 and r_3 axes; (b) as stereographic projection in the complex w plane; (c) as graphs of Re $w(\theta)$ (full curve) and Im $w(\theta)$ (dotted curve); (d) antipodal stereographic projection $-1/w^*$.

as θ approaches 2π. For $w_-(\theta)$, the opposite happens: as θ increases from 0, the exact solution immediately separates from the adiabatic semicircle, on a complicated track, but they both come close together at $\theta = 2\pi$.

As a first step towards explaining these tracks, we calculate the large ρ asymptotic behaviour of the final polarizations for the initial states (4.2), using the exact formula (3.9) and standard large-argument asymptotic formulae for the Bessel functions (see section 10.17(i) of [23]). This leads to

$$w_-(2\pi) \approx \sqrt{\rho} - \tfrac{1}{4}\mathrm{i}(1 + \exp(8\mathrm{i}\sqrt{\rho}))$$
$$w_+(2\pi) \approx -\sqrt{\rho}\frac{(1 - 2\mathrm{i}\exp(-4\mathrm{i}\sqrt{\rho}))}{(1 + 2\mathrm{i}\exp(-4\mathrm{i}\sqrt{\rho}))}\,. \qquad (4.3)$$

These formulae show that as ρ increases the polarization track for $w_-(\theta)$ approaches the south pole on the sphere, and with Re $w_- > 0$, in accordance with adiabatic intuition based on the flip (cf (4.1)); the approach is accompanied by diminishing oscillations. But for $w_+(\theta)$ the approach, although again towards the south pole as expected, also has Re $w_+ > 0$, whereas flip intuition (cf (4.1)) would predict Re $w_+ < 0$; moreover the approach is accompanied by larger oscillations. As figures 4 and 5 illustrate, these predictions based on (4.3) are accurate, even when ρ is not large.

The reason for the failure of naive adiabatic intuition is the Stokes phenomenon of asymptotics. This is the rapid appearance in a function, as a parameter varies, of an exponentially small contribution while this is hidden behind a large one [17, 25, 26]. The detailed mechanism of the birth of the small exponential (switching on according to an error function) is well understood in general [27, 28] and has been described for the non-Hermitian evolution of the model we are exploring [12]. But the mechanism is less important for polarization evolution and we do not consider it further.

For the polarization states considered here, the exponentials occur in the components $\psi_1(\theta)$ and $\psi_2(\theta)$, whose quotient, according to (2.9), is $w(\theta)$. As explained fully elsewhere [12], for the model (3.1) the exponential in the components of the adiabatic state $w_{\mathrm{ad}+}(\theta)$ in (4.1) is dominant during the cycle $0 < \theta < 2\pi$, and that of the state $w_{\mathrm{ad}-}(\theta)$ is subdominant. The two exponentials, involving $\zeta(\theta)$ as defined in (3.6), are [12]

$$\exp(\mp\mathrm{i}\zeta(\theta)) = \exp(\mp 2\mathrm{i}\sqrt{\rho}\exp(\tfrac{1}{2}\mathrm{i}\theta)) \qquad \text{for } w_{\pm\mathrm{ad}}(\theta). \qquad (4.4)$$

Maximal dominance of $w_{\mathrm{ad}+}$ over $w_{\mathrm{ad}-}$ occurs in the middle of the cycle, i.e. $\theta = \pi$.

Consider now the exact state $w_+(\theta)$, with initial polarization $w_{0\mathrm{ad}+}$. This will evolve into a linear combination of the $w_{\mathrm{ad}+}(\theta)$ and $w_{\mathrm{ad}-}(\theta)$ eigenpolarizations, whose multipliers (considered in detail in [12]), will be almost constant except near $\theta = \pi$. There, the multiplier of $w_{\mathrm{ad}-}(\theta)$ will change rapidly from zero to 2i, in which 2i is the Stokes

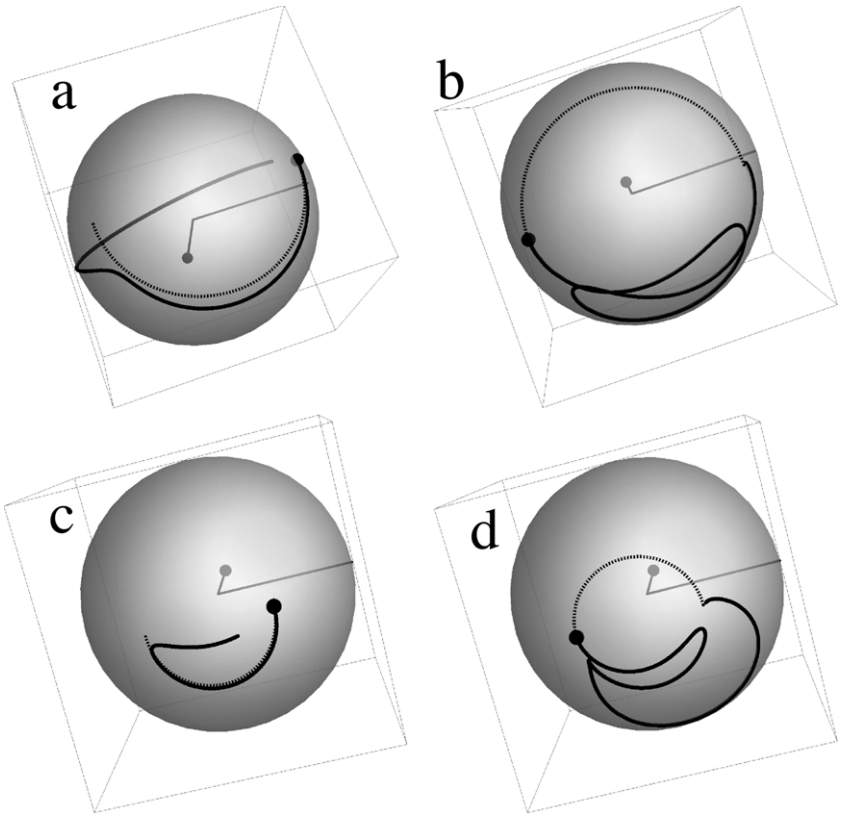

Figure 3. Poincaré sphere tracks of polarization evolutions starting from adiabatic initial conditions (4.2), for (a) $\rho = 4$, +state; (b) $\rho = 4$, −state; (c) $\rho = 20$, +state; (d) $\rho = 20$, −state. The full curves show the exact evolutions calculated from (3.5) to (3.7) and the dotted curves show the evolving local eigenpolarizations (4.1). Filled circles mark the initial polarizations and the north pole, and straight lines indicate the positive r_1 and r_3 axes. In this and subsequent figures, the spheres are oriented to give the clearest views of the polarization tracks.

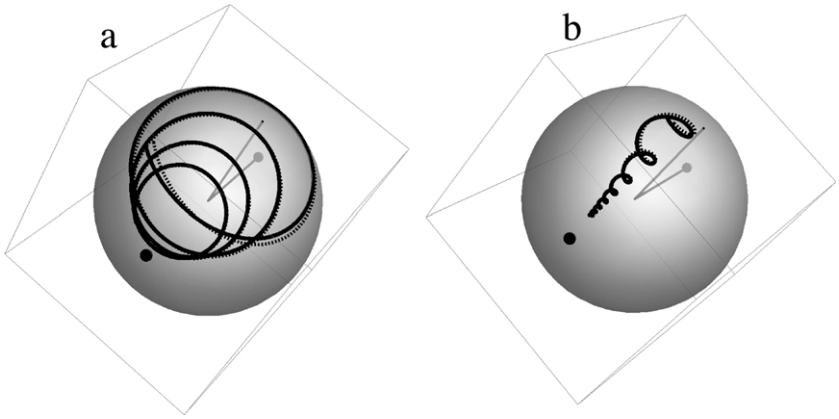

Figure 4. Final polarization states on Poincaré sphere as functions of loop radius, for $1 \leqslant \rho \leqslant 50$ and adiabatic initial states (4.2), for (a) $w_+(2\pi)$; (b) $w_-(2\pi)$. Full curves: exact final states from (3.9); dotted curves: asymptotic approximation (4.3). Filled circles indicate the north and south poles.

constant for the zero-order Bessel functions [29], as embodied in the continuation formula for Y_0 in (3.8).

The simplest formula for the component $\psi_1(\theta)$ that incorporates this insight is

$$\psi_1(\theta) \approx \exp(-\mathrm{i}\zeta(\theta)) + 2\mathrm{i}\Theta(\theta - \pi)\exp(\mathrm{i}\zeta(\theta)), \qquad (4.5)$$

in which the smooth switching-on [27] of $w_{\mathrm{ad}-}(\theta)$ is approximated by the step function Θ. For our model, the component $\psi_2(\theta)$ is simply the derivative of $\psi_1(\theta)$ (cf (2.7), (3.1) and (3.5)). Thus, ignoring the derivative of the smooth switching caricatured by the step function, which occurs where this contribution is exponentially small, we find

$$\psi_2(\theta) = \partial_\theta \psi_1(\theta)$$
$$\approx \sqrt{\rho}\exp(\tfrac{1}{2}\mathrm{i}\theta)[\exp(-\mathrm{i}\zeta(\theta)) - 2\mathrm{i}\Theta(\theta - \pi)\exp(\mathrm{i}\zeta(\theta))]. \qquad (4.6)$$

Table 1. Coefficients a_n determined by (5.2).

n	0	1	2	3	4	5	6	7	8
a_n	1	$-\frac{1}{4}\mathrm{i}$	$\frac{1}{32}$	$\frac{1}{64}\mathrm{i}$	$-\frac{25}{2048}$	$-\frac{13}{1024}\mathrm{i}$	$\frac{1073}{65\,536}$	$\frac{103}{4096}\mathrm{i}$	$-\frac{375\,733}{8\,338\,608}$

For the polarization, this gives

$$w_+(\theta) \approx w_{\mathrm{Stokes}}(\theta) = \sqrt{\rho}\exp\left(\frac{1}{2}\mathrm{i}\theta\right)\frac{(1-2\mathrm{i}\Theta(\theta-\pi)\exp(4\mathrm{i}\sqrt{\rho}\exp(\frac{1}{2}\mathrm{i}\theta)))}{(1+2\mathrm{i}\Theta(\theta-\pi)\exp(4\mathrm{i}\sqrt{\rho}\exp(\frac{1}{2}\mathrm{i}\theta)))}. \tag{4.7}$$

This approximation explains the polarization evolution of $w_+(\theta)$: clinging to $w_{\mathrm{ad}+}(\theta)$ not only up to $\theta = \pi$ but also considerably beyond. The reason is that the exponentials involving ρ, which switch on at the middle of the cycle, are negligible except very close to the end of the cycle, where they dominate (reproducing the first formula in (4.3)). And the formula is quite accurate, as figure 6 illustrates. (For the ρ values shown, the exponentially small discontinuities at $\theta = \pi$ are invisible; even for $\rho = 1$ the jump is only of order $\exp(-4)$.) Again the different representations convey different information. In particular, the very large polarization excursions at the end of the cycle are more evident on the Poincaré sphere pictures than on the graphs of $\mathrm{Re}\, w_+(\theta)$ and $\mathrm{Im}\, w_+(\theta)$.

For the state $w_-(\theta)$, with initial polarization $w_{0\mathrm{ad}-}$, the situation is more subtle. Since $w_{\mathrm{ad}-}(\theta)$ is subdominant, there is no Stokes phenomenon at the lowest order of approximation. But a small admixture of $w_{0\mathrm{ad}+}(\theta)$ soon enters, and its exponential quickly dominates as θ increases from zero, causing the large deviations from adiabaticity observed in figures 3(b) and (d). This dominance fades as θ approaches 2π and the exponentials become pure phase factors, so the final polarization state is close to that expected adiabatically, i.e. $+\sqrt{\rho}$. (There will be a weak Stokes jump in the subdominant state, arising from the small admixture of $w_{0\mathrm{ad}+}(\theta)$, but its coefficient will be $O(1/\sqrt{\rho})$ so it does not spoil the flip.)

5. Superadiabatic polarization clinging

Some of the dramatic violations of adiabaticity can be tamed, and insight gained, by comparing the exact evolution with 'superadiabatic' [27] approximations, incorporating corrections to the local eigenpolarizations (4.1). These can be obtained using known Bessel asymptotics as was done in [12], but here, where we are interested only in the polarization, it is simpler and more transparent to solve the governing equation (3.4) directly, as a series in descending powers of ρ (this amounts to studying the logarithm of the usual Bessel or WKB series). The Nth superadiabatic polarization evolution is the truncation of the series to N terms.

The required form of the series is easily found to be

$$w_{\mathrm{ad}\pm}(\theta, N) = \pm\sqrt{\rho}\exp(\tfrac{1}{2}\mathrm{i}\theta) \times \sum_{n=0}^{N} a_n\left(\frac{\pm 1}{\sqrt{\rho}}\right)^n \exp\left(-\frac{1}{2}\mathrm{i}n\theta\right), \tag{5.1}$$

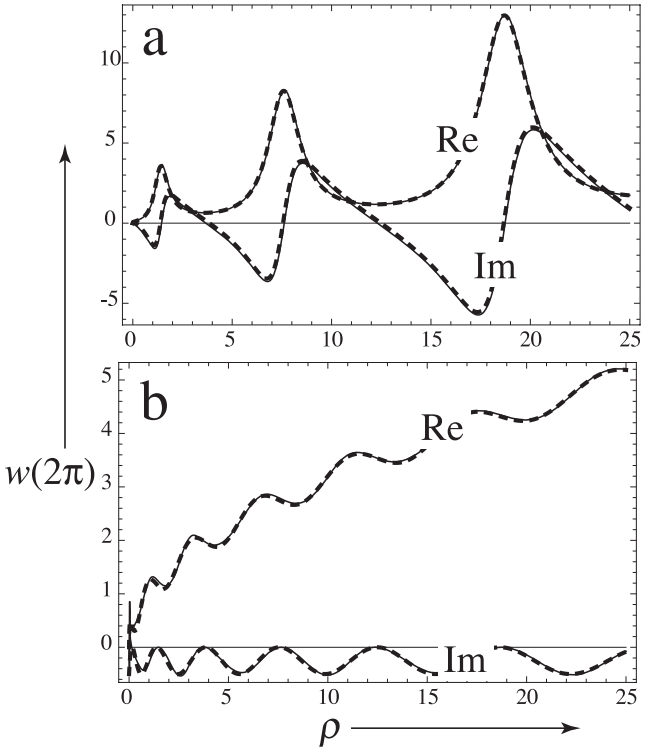

Figure 5. Graphs of real and imaginary parts of final polarization states as functions of loop radius, for (a) $w_+(2\pi)$; (b) $w_-(2\pi)$. Full curves: exact final states from (3.9); dashed curves: asymptotic approximations (4.3).

with the coefficients determined by the following recursion relation, obtained by substitution into (3.2):

$$a_0 = 1, \qquad a_n = \tfrac{1}{2}\left(\mathrm{i}(\tfrac{1}{2}n-1)a_{n-1} - \sum_{m=1}^{n-1} a_m a_{n-m}\right). \tag{5.2}$$

Table 1 shows the first few coefficients.

The infinite series corresponding to (5.1) without truncation is divergent—a fact which, as is well known [18], lies at the heart of the Stokes phenomenon. The precise form of the divergence is described by the following 'asymptotics of the asymptotics' [28], which approximates the coefficients very accurately for large n:

$$a_n \approx -\frac{2\,(n-1)!}{\pi(-4\mathrm{i})^n} \qquad \text{for } n \gg 1. \tag{5.3}$$

The powers of $-\mathrm{i}$ determine the value of θ for which all terms in the superadiabatic series have the same sign—a specification of the Stokes phenomenon equivalent to maximal exponential dominance [18]. Inspection of (5.1) shows that, as expected, this occurs at $\theta = \pi$ for $w_{\mathrm{ad}+}(\theta, N)$, and not at all for $w_{\mathrm{ad}-}(\theta, N)$. And the factorials in (5.3) determine the order N^* at which the series (5.1) has its least term, corresponding to optimal truncation. From Stirling's formula,

$$N^* = \mathrm{int}(4\sqrt{\rho} + \tfrac{1}{2}). \tag{5.4}$$

With this machinery, we can investigate how closely the exact evolving polarizations cling to the Nth order

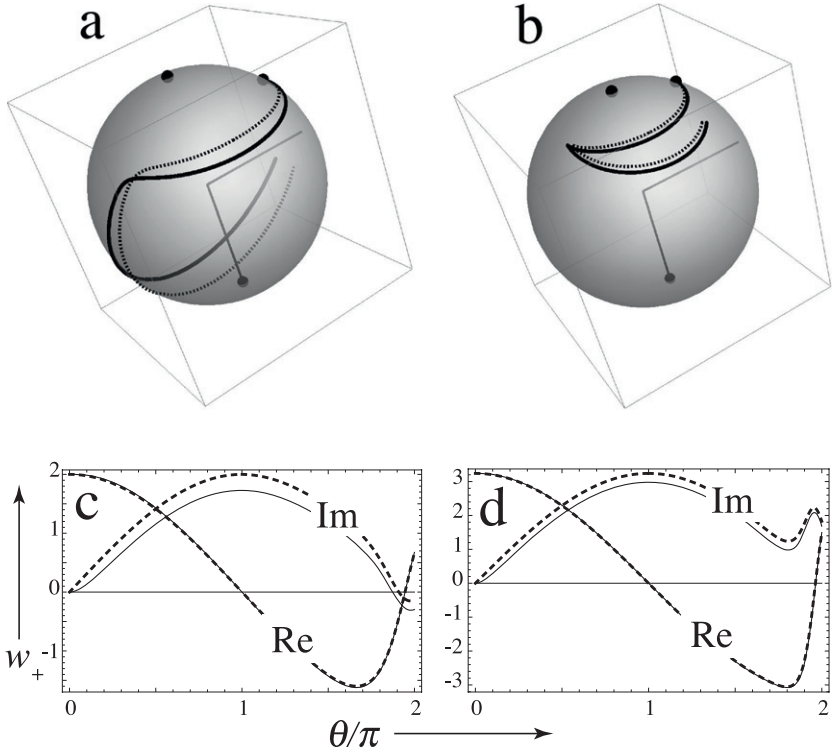

Figure 6. Polarization evolutions for $w_+(\theta)$ for ((a), (c)) $\rho = 4$; ((b), (d)) $\rho = 10.5$. The full curves show the exact evolutions calculated from (3.5) to (3.7) and the dotted curves show the approximation $w_{\text{Stokes}}(\theta)$ given by (4.7). (a), (b) Show tracks on the Poincaré sphere, with filled circles marking the initial polarizations and the north and south poles, and straight lines indicating the positive r_1 and r_3 axes, and ((c) , (d)) are corresponding graphs of Re $w_+(\theta)$ and Im $w_+(\theta)$ as indicated.

superadiabatic polarizations (5.1). To do this, we study the exact evolutions $w_\pm(\theta, N)$ with initial conditions

$$w_\pm(0, N) = w_{0\text{ad}\pm}(N) = w_{\text{ad}\pm}(0, N)$$
$$= \pm\sqrt{\rho}\sum_{n=0}^{N} a_n\left(\frac{\pm 1}{\sqrt{\rho}}\right)^n. \tag{5.5}$$

For $w_+(\theta, N)$, in which the Stokes phenomenon is invisible except near the end of the cycle, this suggests the following simplest modification of (4.7)

$$w_+(\theta, N) \approx w_{\text{Stokes}}(\theta, N) = [(w_{\text{ad}+}(\theta, N) + 2\text{i}\Theta(\theta - \pi)$$
$$\times w_{\text{ad}-}(\theta, N)\exp(4\text{i}\sqrt{\rho}\exp(\tfrac{1}{2}\text{i}\theta)))]$$
$$\times [(1 + 2\text{i}\Theta(\theta - \pi)\exp(4\text{i}\sqrt{\rho}\exp(\tfrac{1}{2}\text{i}\theta)))]^{-1}. \tag{5.6}$$

The effect of this modification, for the first superadiabatic order $N = 1$, is illustrated in figure 7; this should be compared with figure 6 which corresponds to $N = 0$. For most of the cycle—that is before the subdominant exponential contributes significantly, and well beyond $\theta = \pi$—the $N = 1$ approximation is almost indistinguishable from the exact. Close to the end of the cycle, the two evolutions still follow each other; the deviations are smaller than for $N = 0$ but distinguishable, an effect that appears more clearly in the Poincaré tracks of figures 7(a) and (b) than the graphs of figures 7(c) and (d).

The evolution of $w_-(\theta, N)$, in which there is no Stokes phenomenon to lowest order, is illustrated for two values of ρ and increasing superadiabatic order N in figures 8(a), (b) and 9(a), (b). Three features are immediately apparent. First, the evolutions change wildly from one order to the next, illustrating that the polarization evolution for $w_-(\theta)$ is exquisitely sensitive to initial conditions. Between successive orders of approximation, the initial conditions change by an amount corresponding to the following angle on the Poincaré sphere:

$$|\delta \boldsymbol{r}_0| = |\boldsymbol{r}_0(\theta, n+1) - \boldsymbol{r}_0(\theta, n)| \sim \frac{a_{n+1}}{\rho^{(n+1)/2}}. \tag{5.7}$$

An illustrative example is the utterly different evolutions between orders 6 and 9 on figures 8(b) and 9(b): the initial conditions are separated by an angle of order 2.71×10^{-7} rad $= 0.056$ arcsec (to be compared with the angle $4\arctan(1/\sqrt{20}) \sim 50.4°$ between the two eigenpolarizations). This sensitivity is very state-selective: by contrast, $w_+(\theta, N)$ is relatively robust against perturbation of the initial condition.

Second, as the optimal truncation order N^* is approached, the exact evolutions approach the superadiabatic ones, clinging closely to them for all θ except for an interval near $\theta = \pi$ that gets smaller as ρ increases. Within this interval, the deviations between the exact and superadiabatic evolutions take the form of a series of coils on the Poincaré sphere, and these also get smaller as ρ increases. To describe these coils for optimal truncation N^*, it is necessary to incorporate the contamination of $w_-(\theta, N)$ by the dominant eigenpolarization $w_{\text{ad}+}(\theta, N)$. As explained in appendix C, this is a delicate matter, requiring

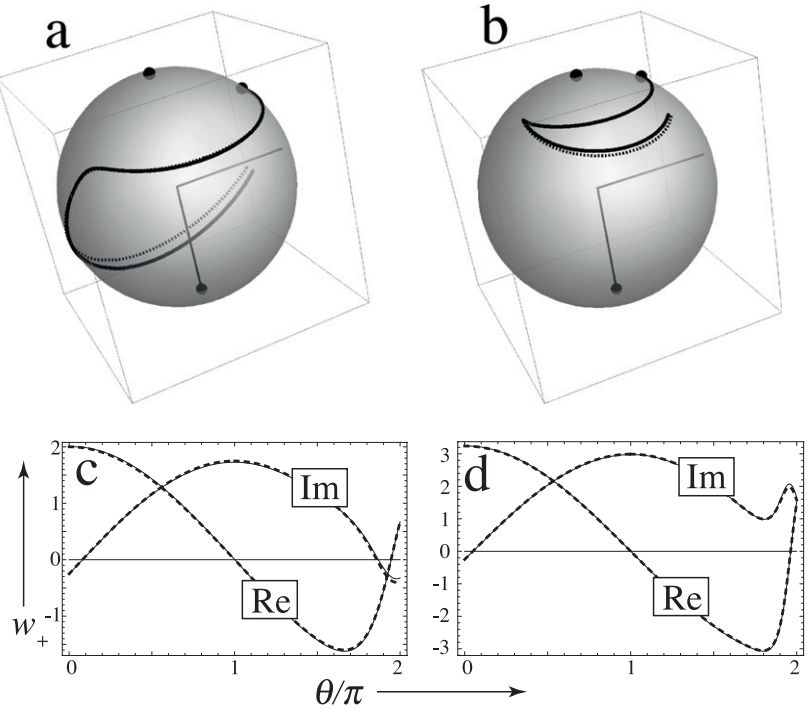

Figure 7. As figure 6, for the first superadiabatically improved approximation, i.e. (5.5) and (5.6) for $N = 1$.

the high-order approximation (5.3) of the coefficients in (5.1). The result is

$$w_-(\theta, N) \approx w_{\rm app}(\theta, N^*)$$
$$= w_{{\rm ad}-}(\theta, N^*) + \frac{1}{\sqrt{\pi}}\rho^{1/4}\exp\left(-8\sqrt{\rho}\sin^2\frac{1}{4}(\theta-\pi)\right)$$
$$\times(-{\rm i})^{N^*}\exp\{{\rm i}(\tfrac{1}{4}\pi + \tfrac{1}{2}\theta + 8\sqrt{\rho}\sin^2\tfrac{1}{4}\theta)\}. \qquad (5.8)$$

Figure 10 illustrates how well this captures the form of the optimal-order polarization coils. Away from $\theta = \pi$, that is away from the loops, the correction term is exponentially smaller than the $w_{{\rm ad}-}$ term, which is of order $\sqrt{\rho}$. Near $\theta = \pi$, it is of order $\rho^{1/4}$, showing how the amplitude of the loops slowly fades as ρ increases.

Third, as the order is increased beyond $N = N^*$, the exact and superadiabatic evolutions separate again, reflecting the divergence of the series (5.1).

6. Concluding remarks

The polarization behaviour described here characterizes propagation in a stratified nontransparent medium whose dielectric properties twist around those of a medium with a singular axis. Mathematically, this is equivalent to the evolution of a vector driven by a non-Hermitian matrix that is cycled, in the space of parameters on which it depends, around a matrix with a branch-point degeneracy (exceptional point). As the polarization tracks illustrate, some aspects of the evolution depend delicately on initial conditions and on other aspects of the medium variation. They join a class of recently predicted qualitatively new polarization phenomena associated with non-Hermitian degeneracies, including interference figures in thin anisotropic [6] and bianisotropic [30] crystal plates, and conical refraction in absorbing biaxial crystals [31, 32].

The loops for which the polarization has been studied here are all centred on the isolated degeneracy at $r = 0$. This is the simplest case. I have not discussed the polarization effects associated with more general loops that are not centred on the degeneracy and may even not enclose it, such as those for which a more general exact solution exists [12]. It would be interesting to do so, in particular to explore the dependence of the state-selective sensitivity on the proximity of the degeneracy to the loop. But to elucidate these effects thoroughly would be a substantial undertaking that would make the paper unreasonably long.

In principle, these effects could be explored experimentally, using a material with the dielectric tensor (A.6). A simplifying feature is the absence of chirality (the dielectric matrix is symmetric). But in practice it might not be easy to identify a corresponding specific material, in which both the transparent and nontransparent anisotropies vary separately along the propagation direction. However, the increasing facility in manufacturing metamaterials with precisely defined properties [33, 34] might make possible the engineering of stratified media such as those in the model studied here, either optically or for microwaves. In any experiment, the intensity must not be so weak as to render the polarization unobservable. According to (2.14), the intensity involves not only the traceless part of the dielectric tensor, represented by $\mathbf{\Omega}(\theta)$, which influences the polarization, but also the imaginary part $T(\theta)$ of the trace of the tensor, which does not. In principle, any intensity variations associated with $\mathbf{\Omega}(\theta)$, that could threaten the observability of the polarization, might be compensated by $T(\theta)$ in a suitably designed metamaterial.

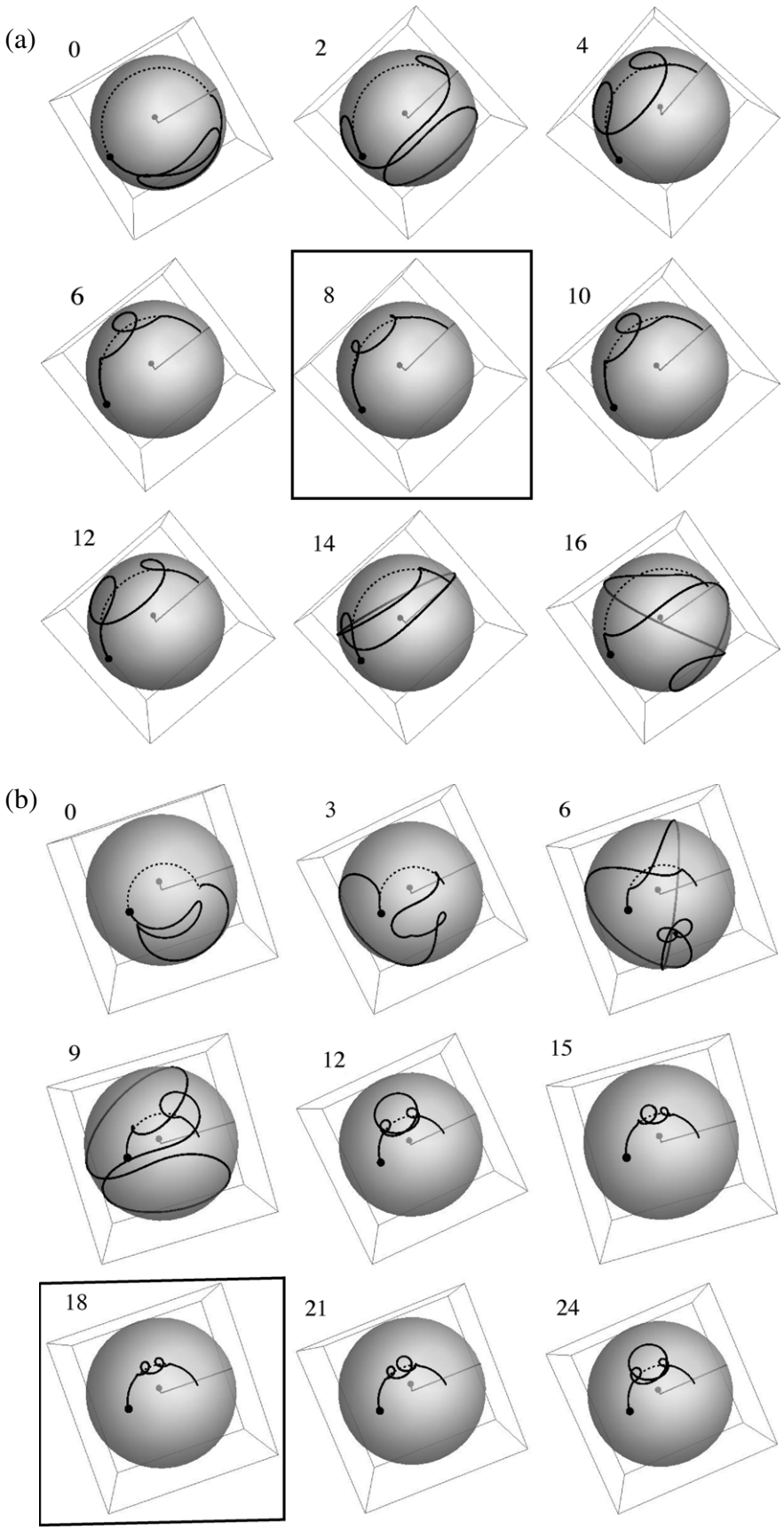

Figure 8. Comparison of exact polarization evolution on the Poincaré sphere for $w_-(\theta, N)$ (full curves), for superadiabatic initial conditions (5.5), with the superadiabatic approximations $w_{\mathrm{ad}-}(\theta, N)$ (equation (5.1)), (dashed curves) for the indicated values of N, illustrating the sensitivity of these evolutions to changing order. The optimal superadiabatic order N^* (equation (5.4)) is highlighted. (a) $\rho = 4$; (b) $\rho = 20$.

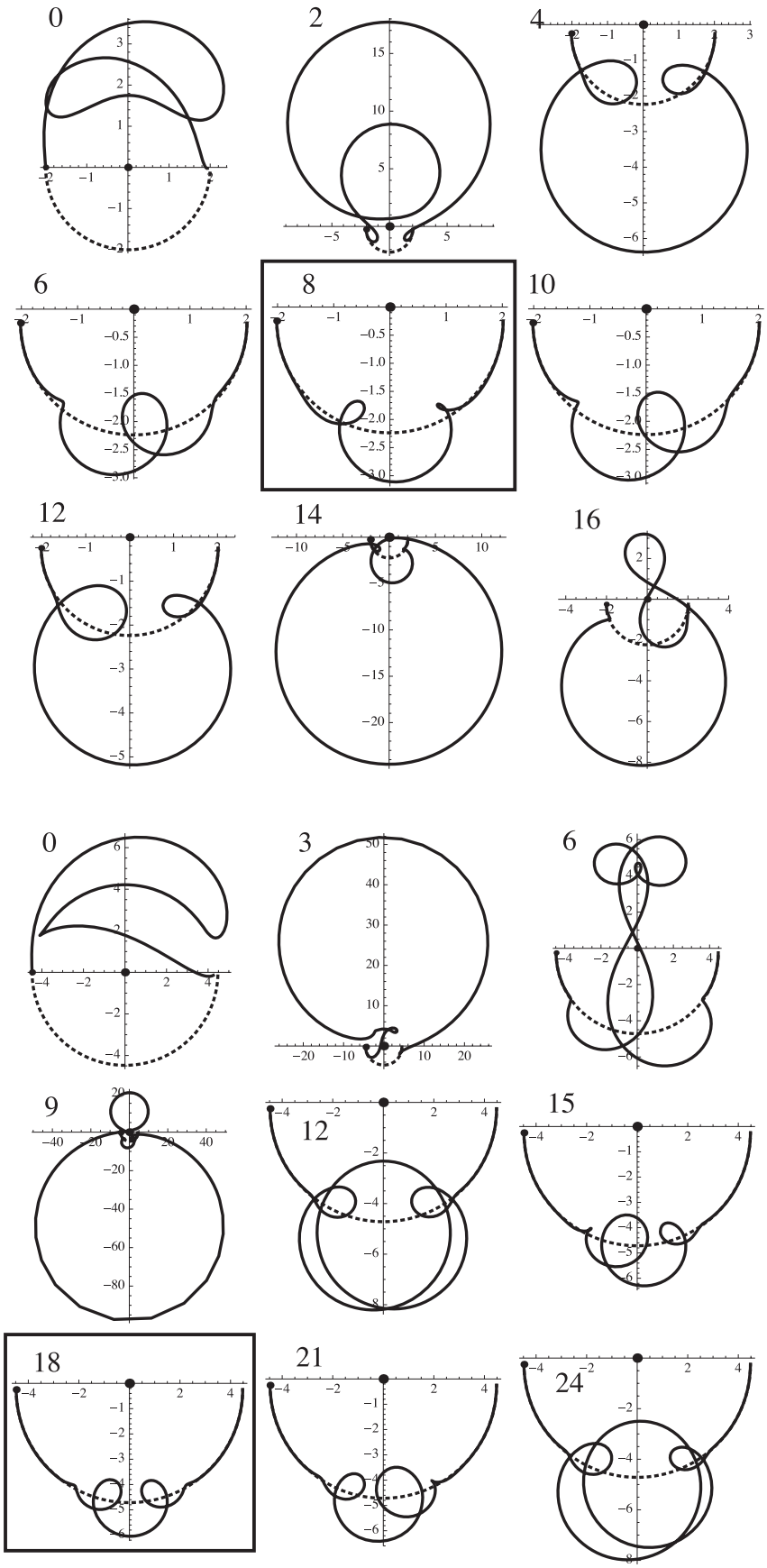

Figure 9. As figure 8, with polarization evolution represented by $w_-(\theta, N)$ in the stereographic plane.

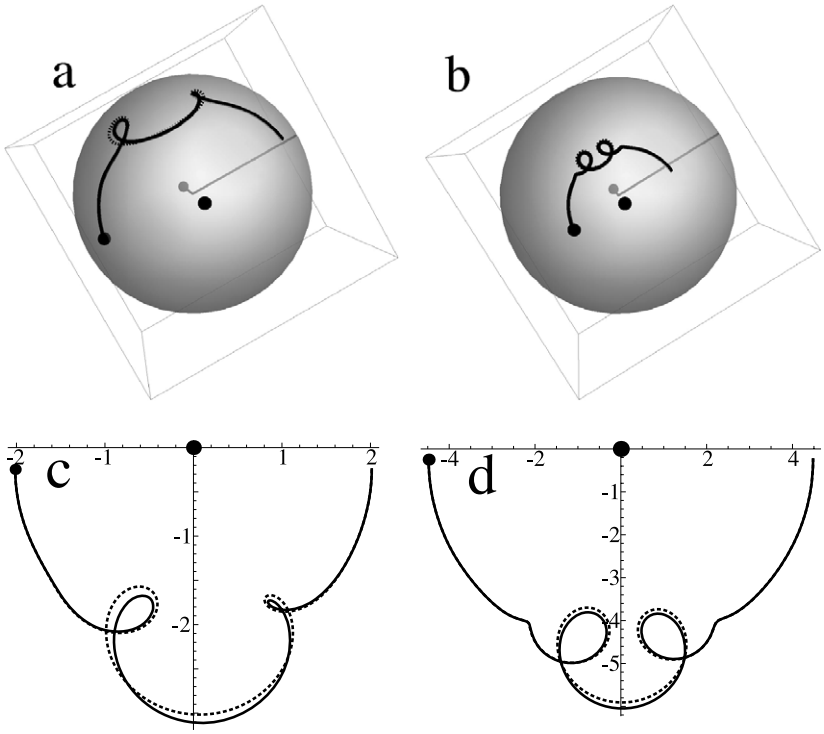

Figure 10. As figures 8 and 9, with the optimal-order exact loops (full curves) compared with the improved approximation (5.8) (dashed curves). (a), (c) $\rho = 4$, $N^* = 8$; (b), (d) $\rho = 20$, $N^* = 18$.

The principal phenomena that are reported here, of evolving states departing from the medium's local eigenpolarizations, even when the stratification is slow, represent extreme violations of adiabatic intuition. As we have seen, the underlying mathematical feature is that of the Stokes phenomenon. This too was discovered [25] in an optical context, namely understanding Airy's integral [35] describing light intensity across a rainbow, and it is worth describing the analogy in more detail.

In the rainbow, light on the dark side is described by a single subdominant exponential—an evanescent wave. Continuing this to the bright side, round a semicircle in the complex plane of a rainbow-crossing variable, this exponential becomes dominant, and at maximal dominance (two-thirds of the way round) the Stokes phenomenon occurs: a second, subdominant, exponential is born. Thereafter one exponential waxes and one wanes, until on the dark side their magnitudes are equal, giving rise to interference in the waves that they represent, visible as the intensity oscillations in supernumerary rainbows [36]. Likewise, in our polarization evolutions of the dominant state $w_+(\theta)$, illustrated in figure 6, the second exponential appears at $\theta = \pi$, where it is subdominant, but it is insignificant until the end of the cycle; there, its interference with the dominant exponential gives rise to the final-state polarization oscillations in figures 4 and 5.

Acknowledgments

I am grateful to Nimrod Moiseyev and Raam Uzdin of the Technion for sharing their discovery [3] before publication, leading to the joint work [12] and thus inspiring the optical application reported here. I also thank Raam Uzdin and two referees for their careful reading of this paper and helpful suggestions.

Appendix A. Non-Hermitian model as perturbation of Hermitian dielectric medium

In the optics of transparent anisotropic crystals, a degeneracy of the 2×2 Hermitian propagation matrix (2.3) corresponds to illumination along an optic axis. When this is perturbed to incorporate dissipation, the matrix becomes non-Hermitian and each optic axis splits into a pair of singular axes [5, 30]. We can mimic this physical behaviour by separating the matrix (3.1) into its Hermitian and anti-Hermitian parts, and then introducing a perturbation parameter ε to make the purely Hermitian part and our non-Hermitian part (3.1) correspond to $\varepsilon = 0$ and $\varepsilon = 1$ respectively. This suggests (using the notation (3.2)) the extended model

$$\mathbf{\Omega}(\theta)\cdot\boldsymbol{\sigma} = \frac{\mathrm{i}\mu}{2}\begin{pmatrix} 0 & -z^* + \varepsilon(2+z^*) \\ (1+\varepsilon)z & 0 \end{pmatrix} \qquad (0 \leqslant \varepsilon \leqslant 1), \tag{A.1}$$

in which the components of the vector $\mathbf{\Omega}(\theta)$ are

$$\Omega_1 = \tfrac{1}{2}\mu(-\rho\sin\theta + \mathrm{i}\varepsilon(1+\rho\cos\theta)), \qquad \Omega_2 = \tfrac{1}{2}\mu(\rho\cos\theta - \varepsilon + \mathrm{i}\varepsilon\rho\sin\theta), \qquad \Omega_3 = 0. \tag{A.2}$$

To understand the reason for the particular choice (A.1) from the many possible model perturbations, note that the eigenvalues of $\mathbf{\Omega}(\theta)\cdot\boldsymbol{\sigma}$ are

$$\lambda = \pm\tfrac{1}{2}\mathrm{i}\mu\sqrt{(1+\varepsilon)(\xi+\mathrm{i}\eta)(2\varepsilon - (\xi-\mathrm{i}\eta)(1-\varepsilon))}. \tag{A.3}$$

The degeneracies—zeros of this function—are at

$$\xi = 0, \qquad \eta = 0, \qquad \text{and}$$
$$\xi = \frac{2\varepsilon}{1-\varepsilon}, \qquad \eta = 0. \tag{A.4}$$

At $\varepsilon = 0$, these coincide, and the origin of the z plane is a diabolical point [37], that is, a degeneracy of the unperturbed Hermitian matrix. As ε increases from zero, this splits into two branch-points: as $\varepsilon \to 1$, one recedes towards infinity, while the other remains at the origin where it can be encircled separately, to generate the polarization evolutions studied in this paper.

Transforming back to the Cartesian representation using (2.6), we find that (A.1) corresponds to a medium with the following variation of the transverse dielectric tensor (cf (2.3)):

$$\delta\boldsymbol{\eta}(\theta) = \delta\boldsymbol{\eta}_0(\theta) + \varepsilon(\delta\boldsymbol{\eta}_1 + \mathrm{i}\delta\boldsymbol{\eta}_1(\theta)), \tag{A.5}$$

where, with Pauli matrices σ_1, σ_3 and rotation matrices R,

$$\delta\boldsymbol{\eta}_0(\theta) = \tfrac{1}{2}\mu\rho R(\tfrac{1}{2}\theta)\sigma_1 R(-\tfrac{1}{2}\theta) = \tfrac{1}{2}\mu\rho\begin{pmatrix} -\sin\theta & \cos\theta \\ \cos\theta & \sin\theta \end{pmatrix}$$
$$\delta\boldsymbol{\eta}_1 = -\tfrac{1}{2}\mu\sigma_1 = -\tfrac{1}{2}\mu\begin{pmatrix} 0 & 1 \\ 1 & 0 \end{pmatrix} \tag{A.6}$$
$$\delta\boldsymbol{\eta}_2(\theta) = \tfrac{1}{2}\mu(\sigma_3 + \rho R(\tfrac{1}{2}\theta)\sigma_3 R(-\tfrac{1}{2}\theta))$$
$$= \tfrac{1}{2}\mu\begin{pmatrix} 1+\rho\cos\theta & \rho\sin\theta \\ \rho\sin\theta & -1-\rho\cos\theta \end{pmatrix}.$$

This represents a biaxial medium with a transparent part whose dielectric tensor is proportional to σ_1 and a nontransparent part whose dielectric tensor is proportional to σ_3. Each of the parts consists of a non-twisted constituent with constant strength and a twisted constituent whose strength is proportional to the loop radius ρ. Because the tensor (A.5) is a symmetric matrix, the polarization explored here could be engineered with a twisted medium that is non-chiral.

Appendix B. Hermitian limit

The Hermitian limit $\varepsilon = 0$ of (A.1) is

$$\boldsymbol{\Omega}\cdot\boldsymbol{\sigma} \to \tfrac{1}{2}\mu\begin{pmatrix} 0 & -\mathrm{i}\rho\exp(-\mathrm{i}\theta) \\ \mathrm{i}\rho\exp(\mathrm{i}\theta) & 0 \end{pmatrix}. \tag{B.1}$$

The corresponding dielectric tensor $\delta\boldsymbol{\eta}_0(\theta)$ in (A.6) could represent a nematic liquid crystal twisted along the beam direction, or, equivalently, an untwisted cholesteric liquid crystal [38]. In quantum physics, it could represent the evolution of a spin driven by a rotating magnetic field [13]. The polarization evolution equation (2.11) is, after the scaling $K\mu\rho \to \rho$,

$$\partial_\theta w = \tfrac{1}{4}\rho(\exp(-\mathrm{i}\theta)w^2 + \exp(\mathrm{i}\theta)). \tag{B.2}$$

As can easily be confirmed, the solution corresponding to initial polarization w_0 is

$$w(\rho,\theta,w_0) = w_0\exp(\mathrm{i}\theta) \times \frac{(\sqrt{\rho^2+4} + (\frac{\rho}{w_0} - 2\mathrm{i})\tan(\frac{1}{4}\theta\sqrt{\rho^2+4}))}{(\sqrt{\rho^2+4} + (2\mathrm{i} - \rho w_0)\tan(\frac{1}{4}\theta\sqrt{\rho^2+4}))}. \tag{B.3}$$

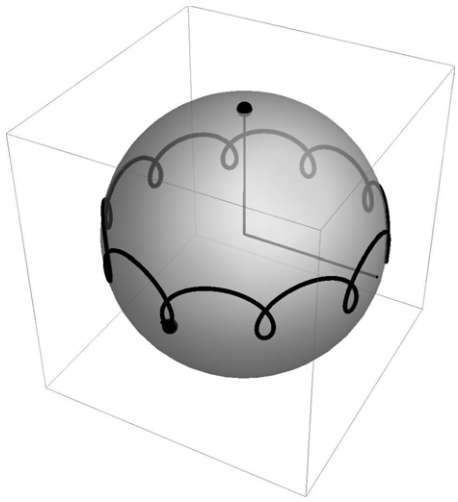

Figure B.1. Hermitian polarization evolution (B.3) on the Poincaré sphere, for $w_0 = -1.086\mathrm{i}$ (indicated by a dot). w_0 is chosen to be 1.2 times w_0 in (B.4) for $\rho = 20$.

Figure B.1 illustrates the evolution for a typical case. It shows that on average the polarization has constant ellipticity (parallels of latitude on the Poincaré sphere), with the direction of the major axis rotating along the beam path. Superimposed on this average evolution are rapid oscillations in the ellipticity. This looks very different from the non-Hermitian evolutions considered in the main body of this paper.

The special periodic (Floquet) solutions, analogous to (3.10), are

$$w_0 = \frac{\mathrm{i}}{\rho}(2 \pm \sqrt{\rho^2+4}), \qquad w(\rho,\theta) = \frac{\mathrm{i}}{\rho}\exp(\mathrm{i}\theta)w_0. \tag{B.4}$$

For these solutions, the polarizations evolve exactly on parallels of latitude, without the oscillations of the typical solutions.

Figure B.1 clearly resembles the precession and nutation of the axis of a spinning top. The periodic solutions (B.4) correspond to the non-nutating 'slow manifold' of dynamics, studied elsewhere [16].

Appendix C. Optimal superadiabatic polarization loops: derivation of (5.8)

From the exact solution in [12], we can write the most general evolving polarization state in a form equivalent to (3.5) but suitable for a perturbation of a state close to the optimal-order subdominant eigenpolarization $w_{\mathrm{ad}-}(\theta, N^*)$ in (5.1):

$$w(\theta) = \partial_\theta\log[H_0^{(1)}(2\sqrt{\rho}\exp(\tfrac{1}{2}\mathrm{i}\theta)) + \varepsilon H_0^{(2)}(2\sqrt{\rho}\exp(\tfrac{1}{2}\mathrm{i}\theta))]$$
$$= \partial_\theta\log\Big[H_0^{(1)}(2\sqrt{\rho}\exp(\tfrac{1}{2}\mathrm{i}\theta)) \times\Big(1 + \varepsilon\frac{H_0^{(2)}(2\sqrt{\rho}\exp(\tfrac{1}{2}\mathrm{i}\theta))}{H_0^{(1)}(2\sqrt{\rho}\exp(\tfrac{1}{2}\mathrm{i}\theta))}\Big)\Big]. \tag{C.1}$$

Here $H_0^{(1)}$ is the subdominant Bessel function and $H_0^{(2)}$ is the dominant state that is contaminating it, with ε representing

the strength of contamination, which arises from the fact that the superadiabatic initial conditions (5.5) are not exactly those corresponding to $H_0^{(1)}$.

The main term can be written, formally, as the infinite superadiabatic series correcting $w_{\mathrm{ad}-}(\theta, N^*)$, that is,

$$\begin{aligned}
&\partial_\theta \log H_0^{(1)}(2\sqrt{\rho}\exp(\tfrac{1}{2}\mathrm{i}\theta)) \\
&= -\sqrt{\rho}\exp\left(\frac{1}{2}\mathrm{i}\theta\right)\sum_{n=0}^{\infty} a_n\left(\frac{-1}{\sqrt{\rho}}\right)^n \exp\left(-\frac{1}{2}\mathrm{i}n\theta\right) \\
&= w_{\mathrm{ad}-}(\theta, N^*) - \sqrt{\rho}\exp(\tfrac{1}{2}\mathrm{i}\theta) \\
&\quad \times \sum_{n=N*+1}^{\infty} a_n\left(\frac{-1}{\sqrt{\rho}}\right)^n \exp\left(-\frac{1}{2}\mathrm{i}n\theta\right) \qquad \text{(C.2)}
\end{aligned}$$

in which the optimal-order superadiabatic series has been separated from its associated formally divergent tail. For the correction term in ε we have, to lowest order, using standard Bessel asymptotics,

$$\begin{aligned}
&\varepsilon\partial_\theta \frac{H_0^{(2)}(2\sqrt{\rho}\exp(\frac{1}{2}\mathrm{i}\theta))}{H_0^{(1)}(2\sqrt{\rho}\exp(\frac{1}{2}\mathrm{i}\theta))} \\
&\quad \approx 2\mathrm{i}\varepsilon\sqrt{\rho}\exp(\tfrac{1}{2}\mathrm{i}\theta - 4\mathrm{i}\sqrt{\rho}\exp(\tfrac{1}{2}\mathrm{i}\theta)). \qquad \text{(C.3)}
\end{aligned}$$

At $\theta = 0$ this term must cancel the tail of the series in (C.2), leaving the optimal superadiabatic initial condition (5.5) for the evolution $w_-(\theta, N)$ that we are studying. Thus ε is determined by

$$2\mathrm{i}\varepsilon\sqrt{\rho}\exp(-4\mathrm{i}\sqrt{\rho}) = \sqrt{\rho}\sum_{n=N*+1}^{\infty} a_n\left(\frac{-1}{\sqrt{\rho}}\right)^n. \qquad \text{(C.4)}$$

Roughly, the tail of the series is of the same order as its first term (that is, $n = N^* + 1$), but to get the form of the polarization loops we need a more precise estimate. This is based on the formula (5.3) for the high-order coefficients, and the observation that at $\theta = 0$ all the terms do not have the same phase, so there is no Stokes phenomenon. Then we can use Borel summation [18], in the form applicable to optimal truncation, that is

$$\begin{aligned}
&\sum_{n=N*+1}^{\infty} \frac{(n-1)!}{(\mathrm{i}x)^n} \approx \frac{(N^*)!}{(\mathrm{i}x)^{N*+1}} \frac{\exp(-\frac{1}{4}\mathrm{i}\pi)}{\sqrt{2}} \\
&\quad \text{for } N^* \approx \mathrm{int}\, x. \qquad \text{(C.5)}
\end{aligned}$$

Applying this to (C.4) we find ε, and then we get (5.8) after substituting into $w(\theta)$ in (C.1) for general θ, using (C.2) (with the tail neglected because it is insignificant compared with the ε term except near $\theta = 0$), and (C.3), and finally using Stirling's formula for $N^*!$.

References

[1] Moiseyev N 2011 *Non-Hermitian Quantum Mechanics* (Cambridge: University Press)

[2] Berry M V 2004 Physics of nonhermitian degeneracies *Czech. J. Phys.* **54** 1040–7

[3] Uzdin R, Mailybaev A and Moiseyev N 2011 On the observability and asymmetry of adiabatic state flips generated by exceptional points *J. Phys. A.: Math. Theor.* at press

[4] Kato T 1950 On the adiabatic theorem of quantum mechanics *J. Phys. Soc. Japan* **5** 435–9

[5] Ramachandran G N and Ramaseshan S 1961 *Crystal Optics in Handbuch der Physik* vol XXV/I, ed H Flügge (Berlin: Springer)

[6] Berry M V and Dennis M R 2003 The optical singularities of birefringent dichroic chiral crystals *Proc. R. Soc.* A. **459** 1261–92

[7] Born M and Fock V A 1928 Beweis des adiabatensatzes *Z. Phys.* **51** 165–9

[8] Messiah A 1962 *Quantum Mechanics* (Amsterdam: North-Holland)

[9] Born M and Wolf E 2005 *Principles of Optics* (London: Pergamon)

[10] Brosseau C 1998 *Fundamentals of Polarised Light: A Statistical Optics Approach* (New York: Wiley)

[11] Poincaré H 1892 *Théorie Mathématique de la Lumière II* (Paris: George Carré) Reprinted by Éditions Jacques Gabay 1995

[12] Berry M V and Uzdin R 2011 Slow nonhermitian cycling: exact solutions and the Stokes phenomenon *J. Phys. A: Math Theor.* at press

[13] Rabi I I 1937 Space quantization in a gyrating magnetic field *Phys. Rev.* **51** 652–4

[14] Klein F and Sommerfeld A 2008 *The Theory of the Top* vol I *Introduction to the Kinematics and Kinetics of the Top Translators* ed R J Nagen and G Sandri (Boston: Birkhäuser) Originally published by Teubner 1897

[15] Klein F and Sommerfeld A 2010 *The Theory of the Top* vol II *Development of the Theory in the Case of the Heavy Symmetric Top* ed R J Nagen and G Sandri (Boston: Birkhäuser) Originally published by Teubner 1898

[16] Berry M V and Shukla P 2011 Slow manifold and Hannay angle for the spinning-op *Eur. J. Phys.* **32** 115–27

[17] Heading J 1962 *An Introduction to Phase-Integral Methods* (London: Methuen)

[18] Dingle R B 1973 *Asymptotic Expansions: Their Derivation and Interpretation* (New York: Academic)

[19] Berry M V 1990 Histories of adiabatic quantum transitions *Proc. R. Soc. Lond.* **A429** 61–72

[20] Lim R and Berry M V 1991 Superadiabatic tracking for quantum evolution *J. Phys. A: Math. Gen.* **24** 3255–64

[21] Berry M V, Bhandari R and Klein S 1999 Black plastic sandwiches demonstrating biaxial optical anisotropy *Eur. J. Phys.* **20** 1–14

[22] Berry M V, Dennis M R and Lee R L J 2004 Polarization singularities in the clear sky *New J. Phys.* **6** 162

[23] DLMF 2010 *NIST Handbook of Mathematical Functions* (Cambridge: University Press) http://dlmf.nist.gov

[24] Needham T 1997 *Visual Complex Analysis* (Oxford: University Press)

[25] Stokes G G 1864 On the discontinuity of arbitrary constants which appear in divergent developments *Trans. Camb. Phil. Soc.* **10** 106–28

[26] Stokes C G 1902 On the discontinuity of arbitrary constants that appear as multipliers of semi-convergent series *Acta Math.* **24** 393–7

[27] Berry M V 1989 Uniform asymptotic smoothing of Stokes's discontinuities *Proc. R. Soc. Lond.* **A422** 7–21

[28] Berry M V 1989 Stokes' phenomenon; smoothing a Victorian discontinuity *Inst. H. Études Sci. Publ. Math.* **68** 211–21

[29] Olde Daalhuis A B and Olver F W J 1995 On the calculation of Stokes multipliers for linear differential equations of the second order *Methods Appl. Anal.* **2** 348–67

[30] Berry M V 2005 The optical singularities of bianisotropic crystals *Proc. R. Soc.* A **461** 2071–98

[31] Berry M V and Jeffrey M R 2006 Conical diffraction complexified: dichroism and the transition to double refraction *J. Opt.* A **8** 1043–51
[32] Jeffrey M R 2007 The spun cusp complexified: complex ray focusing in chiral conical diffraction *J. Opt.* **9** 634–41
[33] Benisty H and Weisbuch C 2006 Photonic crystals *Prog. Opt.* **49** 177–213
[34] Sakoda K and Haus J W 2010 Science and engineering of photonic crystals *Prog. Opt.* **54** 271–317
[35] Airy G B 1838 On the intensity of light in the neighbourhood of a caustic *Trans. Camb. Phil. Soc.* **6** 379–403
[36] Lee R and Fraser A 2001 *The Rainbow Bridge: Rainbows in Art, Myth and Science* (Bellingham, WA: Pennsylvania State University and SPIE press)
[37] Berry M V and Wilkinson M 1984 Diabolical points in the spectra of triangles *Proc. R. Soc. Lond.* **A392** 15–43
[38] de Gennes P G 1974 *The Physics of Liquid Crystals* (Oxford: University Press)